UC San Diego
UC San Diego Previously Published Works

Title

Targeting altered cancer methionine metabolism with recombinant methioninase (rMETase) overcomes partial gemcitabine-resistance and regresses a patient-derived orthotopic xenograft (PDOX) nude mouse model of pancreatic cancer

Authors

Kawaguchi, Kei
Miyake, Kentaro
Han, Qinghong
et al.

Peer reviewed

Taylor & Francis
Taylor & Francis Group

REPORT

Check for updates
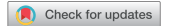
Targeting altered cancer methionine metabolism with recombinant methioninase (rMETase) overcomes partial gemcitabine-resistance and regresses a patient-derived orthotopic xenograft (PDOX) nude mouse model of pancreatic cancer

Kei Kawaguchi[a,b,c], Kentaro Miyake[a,b], Qinghong Han[a], Shukuan Li[a], Yuying Tan[a], Kentaro Igarashi[a,b], Thinzar M. Lwin[a], Takashi Higuchi[a,b], Tasuku Kiyuna[a,b], Masuyo Miyake[a,b], Hiromichi Oshiro[a,b], Michael Bouvet[b], Michiaki Unno[c] and Robert M. Hoffman[a,b]

[a]AntiCancer, Inc., San Diego, CA; [b]Department of Surgery, University of California, San Diego, CA; [c]Department of Surgery, Graduate School of Medicine, Tohoku University, Sendai, Japan

ABSTRACT

Pancreatic cancer is a recalcitrant disease. Gemcitabine (GEM) is the most widely-used first-line therapy for pancreatic cancer, but most patients eventually fail. Transformative therapy is necessary to significantly improve the outcome of pancreatic cancer patients. Tumors have an elevated requirement for methionine and are susceptible to methionine restriction. The present study used a patient-derived orthotopic xenograft (PDOX) nude mouse model of pancreatic cancer to determine the efficacy of recombinant methioninase (rMETase) to effect methionine restriction and thereby overcome GEM-resistance. A pancreatic cancer obtained from a patient was grown orthotopically in the pancreatic tail of nude mice to establish the PDOX model. Five weeks after implantation, 40 pancreatic cancer PDOX mouse models were randomized into four groups of 10 mice each: untreated control (n = 10); GEM (100 mg/kg, i.p., once a week for 5 weeks, n = 10); rMETase (100 units, i.p., 14 consecutive days, n = 10); GEM+rMETase (GEM: 100 mg/kg, i.p., once a week for 5 weeks, rMETase: 100 units, i.p., 14 consecutive days, n = 10). Although GEM partially inhibited PDOX tumor growth, combination therapy (GEM+rMETase) was significantly more effective than mono therapy (GEM: $p = 0.0025$, rMETase: $p = 0.0010$). The present study is the first demonstrating the efficacy of rMETase combination therapy in a pancreatic cancer PDOX model to overcome first-line therapy resistance in this recalcitrant disease.

Introduction

Pancreatic cancer is a recalcitrant disease. Gemcitabine (GEM) is the most widely-used first-line therapy, but most patients eventually fail. Transformative therapy is necessary to significantly improve the outcome of pancreatic cancer patients.

Altered cancer metabolism is currently being investigated for targets for effective novel therapeutics [1]. A very promising candidate target is the elevated methionine (MET) requirement of cancer cells, termed MET dependence. MET dependence may be the only known general metabolic defect in cancer [2–4]. MET dependence is observed when cancer cells selectively arrest upon MET restriction [2–5]. Tumor MET levels correlate with tumor size [6], further demonstrating the dependence of tumors on MET. MET dependence is due to MET overuse by cancer cells [2,5,7,8]. MET overuse can be observed in the clinic by the efficacy of [^{11}C]MET-PET imaging which gives a very strong signal, since the cancer tissue is taking up much more MET than the surrounding normal tissues [9]. MET restriction selectively arrests cancer cells in late S/G$_2$ of the cell cycle where the cancer cells become highly-sensitive to cytotoxic chemotherapy [10–15].

MET is sourced mainly from food. However, MET restriction through diets with low protein content does not allow the maintenance of good nutritional status. In addition, reduction of MET levels by dietary intervention is limited since MET is also sourced from the protein breakdown [2]. In order to more effectively target MET-dependence, we previously cloned *Psuedomonas putida* L-methionine α-deamino-γ-mercaptomethane lyase (recombinant methioniniase [rMETase] [EC 4.4.1.11]) in *E. coli* for large scale industrial production [16–21].

Targeting MET by rMETase arrested growth of cancer cells in vitro and in vivo [21–30]. We previously reported that rMETase, could inhibit tumor growth in patient-derived orthotopic xenograft (PDOX) nude mouse models of melanoma and sarcoma [24–30]. rMETase alone and in combination with a first-line therapy was very effective in the PDOX models [24–30]. For example, rMETase in combination with doxorubicin (DOX) overcame undifferentiated spindle-cell sarcoma (USCS)-resistance to DOX [27,28], which is first line therapy for this disease.

rMETase combined with temozolomide (TEM) [25] was significantly more efficacious than either mono-therapy in a PDOX model of BRAF-V600E mutant melanoma [31–34].

rMETase combined with both tumor-targeting *Salmonella typhimurium* A1-R (*S. typhimurium* A1-R) and cisplatinum (CDDP) eradicated a osteosarcoma PDOX model [29]. Cell-cycle decoy by *S. typhimurium* A1-R, cell-cycle trap by rMETase and cell kill by cisplatinum CDDP was able to eradicate the metastatic osteosarcoma PDOX [29].

In the present study, we utilized a PDOX nude mouse model of pancreatic cancer to demonstrate that rMETase can overcome GEM-resistance.

Results and discussion

GEM alone could inhibit (P = 0.001), but not arrest the pancreatic cancer PDOX. rMETase alone could also inhibit tumor growth (P = 0.020), but not arrest the pancreatic cancer PDOX. In contrast, the combination of GEM+rMETase could regress the pancreatic cancer PDOX ($p < 0.0001$) compared to the untreated control. The combination of GEM+rMETase significantly inhibited tumor growth compared to other treatments. On day-14, GEM: $p = 0.0006$; rMETase: $p = 0.0031$. On day-21: GEM: $p = 0.0215$; rMETase: $p = 0.0001$. On day-28, GEM: $p = 0.0004$; rMETase: $p < 0.0001$). The combination of GEM+rMETase was also significantly more effective than other therapies (GEM: $p = 0.0025$, rMETase: $p = 0.0010$) on day 35 (Figure 1), demonstrating the durability of the response.

Intra-tumor MET levels decreased after rMETase treatment ($p = 0.0060$) (Figure 2). This result showed that the pancreatic cancer PDOX is MET dependent and rMETase has potential to deplete tumor MET.

The body weight on each day, compared with day-0, did not significantly differ between any treatment group (Figure 3).
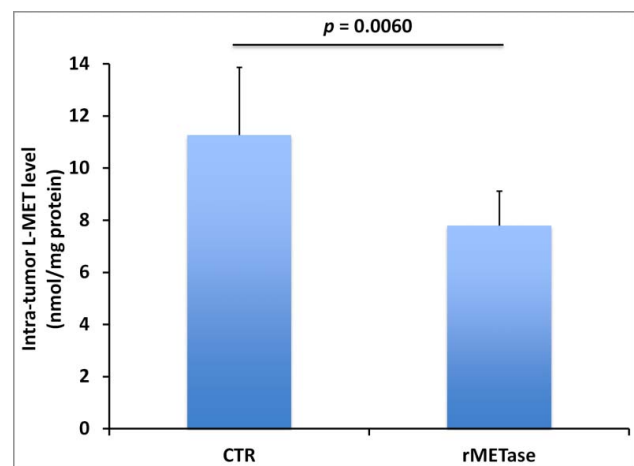
Figure 2. Intra-tumor MET levels. Bar graphs show intra-tumor MET levels in control (CTR) and rMETase-treated tumors. Error bars: ± SD.

There were no animal deaths in any group or untreated control. These results suggest the safety of rMETase and rMETase combination therapy with GEM. Toxicities not indicated by body weight changes may have occurred in the treated groups.

Histologically, the untreated control tumor was mainly comprised of viable cells. In contrast, tumors treated with the combination therapy (GEM+rMETase) showed a great reduction of cancer cells as well as necrosis (Figure 4). It was not possible to determine if all cancer cells were eliminated. GEM-rMETase treatment resulted in the strongest histological effect on the tumors.
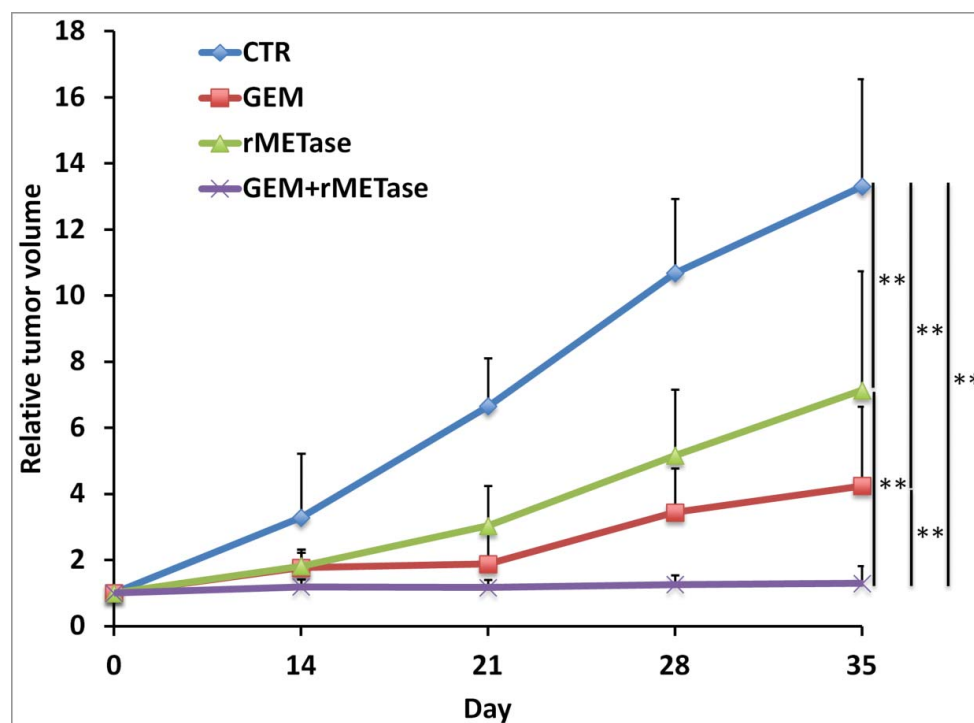
Figure 1. Drug efficacy on the pancreatic cancer PDOX. Line graphs show tumor volume at each point relative to the initial tumor volume for each condition. $^{**}p < 0.01$. Error bars: ± SD.

Figure 3. Effect of treatment on mouse body weight. Bar graphs show mouse body weight in each treatment group at pre- and post-treatment times.

The present report demonstrates that rMETase combination therapy could inhibit pancreatic cancer PDOX growth at least 35 days without overt toxicity. In the GEM+rMETase group, the tumor volume at day-0 was 181 ± 54 mm^3 and at day-35 the tumor volume was 176 ± 80 mm^3. In addition, tumor histology indicated the tumor treated with GEM + rMETase was highly necrotic h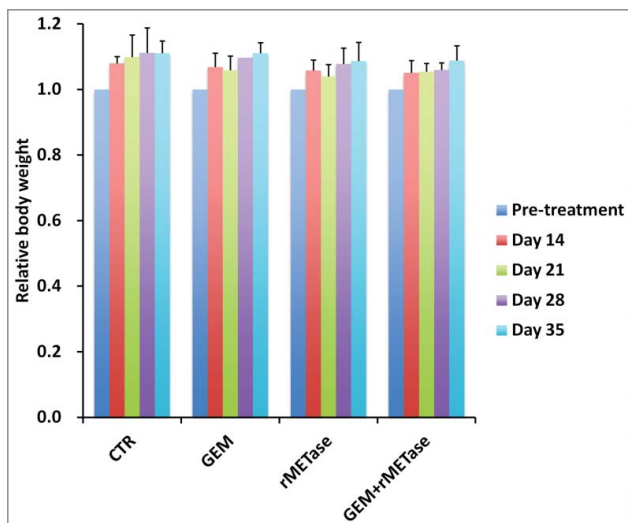as much fewer, if any, cancer cells compared with the tumor at day-0. These results suggest that GEM + rMETase at day-35 has regressed and potentially cured the tumor. These results indicate that GEM combined with rMETase has future clinical potential. The present study demonstrates the power of the PDOX models to identify highly effective therapy for pancreatic cancer, one of the most recalcitrant cancers. The present study indicates that possibly in the near future more effective therapy will be clinically available for pancreatic cancer, which can be identifiable for individual patients using PDOX models.

Using the technique of surgical orthotopic implantation (SOI), PDOX models have been developed for pancreatic [6,35–38], breast [39], ovarian [40], lung [41], cervical [42],

colon [43–45], stomach cancers [46], sarcoma [47–61] and melanoma [25,27,31–33,62], suggesting that improved therapy using rMETase will be developed for all major cancers.

Previously-developed concepts and strategies of highly-selective tumor targeting can take advantage of molecular targeting of tumors, including tissue-selective therapy which focuses on unique differences between normal and tumor tissues [63–68].

Materials and methods

Mice

Athymic *nu/nu* male nude mice (AntiCancer, Inc., San Diego, CA), 4–6 weeks old, were used in this study. All mice were kept in a barrier facility on a high efficiency particulate arrestance (HEPA)-filtered rack under standard conditions of 12-hour light/dark cycles. The animals were fed an autoclaved laboratory rodent diet [26]. All animal experiments were performed with an AntiCancer Institutional Animal Care and Use Committee (IACUC)-protocol specifically approved for this study and in accordance with the principles and procedures outlined in the National Institutes of Health Guide for the Care and Use of Animals under Assurance Number A3873-1. Anesthesia and analgesics were used for all surgical experiments to avoid unnecessary suffering of the mice. Subcutaneous injection of ketamine mixture (a 0.02 ml solution of 20 mg/kg ketamine, 15.2 mg/kg xylazine, and 0.48 mg/kg acepromazine maleate) was used for mice. The response of animals during surgery was monitored carefully to maintain adequate depth of anesthesia. The animals were observed daily and humanely sacrificed by CO_2 inhalation when they met the following criteria: severe tumor burden (more than 20 mm in diameter), prostration, significant body weight loss, difficulty breathing, rotational motion and body temperature drop.

Patient-derived tumor

A patient diagnosed with pancreatic cancer previously had the tumor resected, which was established in nude mice in the MD
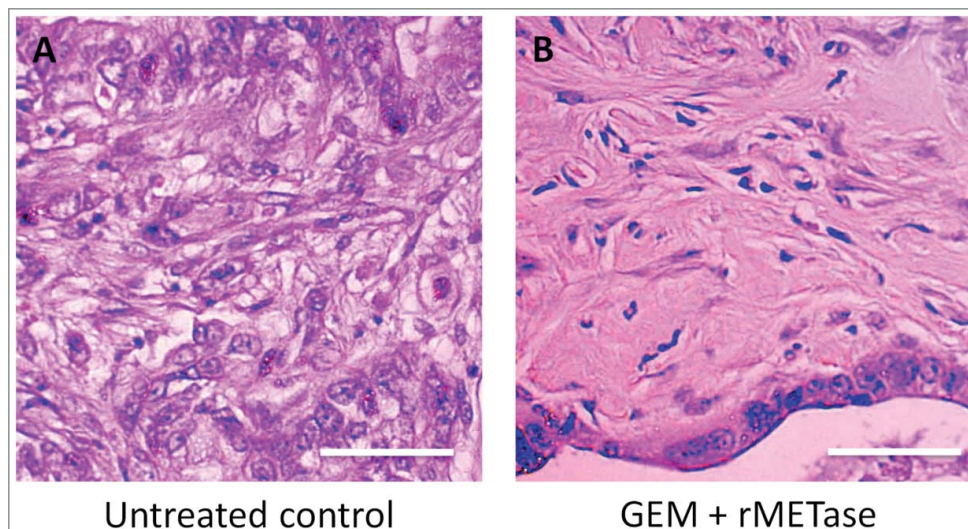
Figure 4. Tumor histology. A. Untreated control. B. Combination treatment with GEM+rMETase. Scale bars: 100 μm.

Anderson Cancer Center. Written informed consent was provided by the patient and the Institutional Review Board (IRB) of MD Anderson Cancer Center approved this experiment [25,26,30–33,69–71].

Surgical orthotopic implantation (SOI)

After nude mice were anesthetized with the ketamine solution described above, a 1–2 cm skin incision was made on the left side abdomen through the skin, fascia and peritoneum and the pancreas was exposed. Surgical sutures (8-0 nylon) were used to implant tumor fragments onto the tail of pancreas to establish the PDOX model. The wound was closed with a 6-0 nylon suture (Ethilon, Ethicon, Inc., NJ, USA) [6,35–38,69–71].

Recombinant methioninase (rMETase) production

Recombinant L-metionine α-deamino-γ-mercaptomethane lyase (recombinant methioninase [rMETase]) [EC 4.4.1.11] from *Pseudomonas putida* has been previously cloned and was produced in *Escherichia coli* (AntiCancer, Inc., San Diego, CA). rMETase is a homotetrameric PLP enzyme of 172-kDa molecular mass [16].

Intra-tumor MET level analysis

At the end of the treatment period, each tumor was sonicated for 30 seconds on ice and centrifuged at 12,000 rpm for 10 minutes. Supernatants were collected and protein levels were measured using the Coomassie Protein Assay Kit (Thermo Scientific, Rockford, IL). Protein levels were calculated from a standard curve obtained with a protein standard, bovine serum albumin (BSA). MET levels were determined with the HPLC procedure described previously [72]. Standardized MET levels were calculated per mg tumor protein [25].

Treatment study design in the PDOX model of pancreatic cancer

PDOX mouse models were randomized into four groups of 10 mice each: untreated control; GEM (100 mg/kg, i.p., once a week for 5 weeks); rMETase (100 units, i.p., 14 consecutive days); GEM+rMETase (GEM: 100 mg/kg, i.p., once a week for 5 weeks, rMETase: 100 units, i.p., 14 consecutive days). Tumor length and width were measured on day 14, 21, 28 and 35. Tumor volume was calculated with the following formula: Tumor volume (mm^3) = length (mm) × width (mm) × width (mm) × 1/2. The data are presented as the tumor volume ratio which is defined at the tumor volume at each point relative to the pre-treatment tumor volume.

Histological examination

Fresh tumor samples were fixed in 10% formalin and embedded in paraffin before sectioning and staining. Tissue sections (5 μm) were deparaffinized in xylene and rehydrated in an ethanol series. Hematoxylin and eosin (H&E) staining was performed according to standard protocols. Histological examination was performed with a BHS System Microscope (Olympus Corporation, Tokyo, Japan). Images were acquired with INFINITY ANALYZE software (Lumenera Corporation, Ottawa, Canada) [25,26,30–33].

Statistical analysis

JMP version 11.0 was used for all statistical analyses. Significant differences for continuous variables were determined using the Mann-Whitney U test. Line graphs express average values and error bars show SD. A probability value of $P \leq 0.05$ was considered statistically significant.

Dedication

This paper is dedicated to the memory of A. R. Moossa, M.D., Sun Lee, M.D. and Shigeo Yagi, Ph.D.

Disclosure of potential conflicts of interest

K.K., K.M., T.H., T.K. and R.M.H. are unsalaried associates of AntiCancer Inc. There are no other competing financial interests.

References

[1] Chong LD. Exploiting cancer metabolism. Science. 2017;355:1036. doi:10.1126/science.355.6329.1036-b. PMID:28280192

[2] Hoffman RM. Development of recombinant methioninase to target the general cancer-specific metabolic defect of methionine dependence: A 40-year odyssey. Expert Opin Biol Ther. 2015;15:21–31. doi:10.1517/14712598.2015.963050. PMID:25439528

[3] Mecham JO, Rowitch D, Wallace CD, et al. The metabolic defect of methionine dependence occurs frequently in human tumor cell lines. Biochem Biophys Res Commun. 1983;117:429–434. doi:10.1016/0006-291X(83)91218-4. PMID:6661235

[4] Tan Y, Xu M, Hoffman RM. Broad selective efficacy of recombinant methioninase and polyethylene glycol-modified recombinant methioninase on cancer cells in vitro. Anticancer Res. 2010;30:1041–1046. PMID:20530407

[5] Hoffman RM, Erbe RW. High in vivo rates of methionine biosynthesis in transformed human and malignant rat cells auxotrophic for methionine. Proc Natl Acad Sci USA. 1976;73:1523–1527. doi:10.1073/pnas.73.5.1523. PMID:179090

[6] Kawaguchi K, Han Q, Li S, et al. Intra-tumor L-methionine level highly correlates with tumor size in both pancreatic cancer and melanoma patient-derived orthotopic xenograft (PDOX) nude-mouse models. Oncotarget. in press.

[7] Coalson DW, Mecham JO, Stern PH, et al. Reduced availability of endogenously synthesized methionine for S-adenosylmethionine formation in methionine dependent cancer cells. Proc Natl Acad Sci USA. 1982;79:4248–4251. doi:10.1073/pnas.79.14.4248. PMID:6289297

[8] Stern PH, Hoffman RM. Elevated overall rates of transmethylation in cell lines from diverse human tumors. In Vitro. 1984;20:663–670. doi:10.1007/BF02619617. PMID:6500606

[9] Xu W, Gao L, Shao A, et al. The performance of 11C-Methionine PET in the differential diagnosis of glioma recurrence. Oncotarget. 2017;8:91030–91039. PMID:29207622

[10] Hoffman RM, Jacobsen SJ. Reversible growth arrest in simian virus 40-transformed human fibroblasts. Proc Natl Acad Sci USA. 1980;77:7306–7310. doi:10.1073/pnas.77.12.7306. PMID:6261250

[11] Stern PH, Hoffman RM. Enhanced in vitro selective toxicity of chemotherapeutic agents for human cancer cells based on a metabolic defect. J Natl Cancer Inst. 1986;76:629–639. doi:10.1093/jnci/76.4.629. PMID:3457200

[12] Guo H, Lishko VK, Herrera H, et al. Therapeutic tumor-specific cell-cycle block induced by methionine starvation *in vivo*. Cancer Res. 1993;53:5676–5679. PMID:8242623

[13] Guo HY, Hoffman RM, Herrera H. Unchecked DNA synthesis and blocked cell division induced by methionine deprivation in a human prostate cancer cell line. In Vitro Cell Dev Biol. 1993;29A:359–361. doi:10.1007/BF02633982.

[14] Yano S, Li S, Han Q, et al. Selective methioninase-induced trap of cancer cells in S/G$_2$ phase visualized by FUCCI imaging confers chemosensitivity. Oncotarget. 2014;5:8729–8736. doi:10.18632/oncotarget.2369. PMID:25238266

[15] Yano S, Takehara K, Zhao M, et al. Tumor-specific cell-cycle decoy by *Salmonella typhimurium* A1-R combined with tumor-selective cell-cycle trap by methioninase overcome tumor intrinsic chemoresistance as visualized by FUCCI imaging. Cell Cycle. 2016;15:1715–1723. doi:10.1080/15384101.2016.1181240. PMID:27152859

[16] Tan Y, Xu M, Tan X, et al. Overexpression and large-scale production of recombinant L-methionine-alpha- deamino-gamma-mercaptomethane-lyase for novel anticancer therapy. Protein Expres Purif. 1997;9:233–245. doi:10.1006/prep.1996.0700. PMID:9056489

[17] Takakura T, Ito T, Yagi S, et al. High-level expression and bulk crystallization of recombinant L-methionine γ-lyase, an anticancer agent. Appl Microbiol Biotechnol. 2006;70:183–192. doi:10.1007/s00253-005-0038-2. PMID:16012835

[18] Takakura T, Takimoto A, Notsu Y, et al. Physicochemical and pharmacokinetic characterization of highly potent recombinant L-methionine γ-lyase conjugated with polyethylene glycol as an antitumor agent. Cancer Res. 2006;66:2807–2814. doi:10.1158/0008-5472.CAN-05-3910. PMID:16510603

[19] Takakura T, Misaki S, Yamashita M, et al. Assay method for antitumor L-methionine γ-lyase: Comprehensive kinetic analysis of the complex reaction with L-methionine. Anal Biochem. 2004;327:233–240. doi:10.1016/j.ab.2004.01.024. PMID:15051540

[20] Kudou D, Misaki S, Yamashita M, et al. Structure of the antitumour enzyme L-methionine γ-lyase from *Pseudomonas putida* at 1.8Å resolution. J Biochem. 2007;141:535–544. doi:10.1093/jb/mvm055. PMID:17289792

[21] Yoshioka T, Wada T, Uchida N, et al. Anticancer efficacy *in vivo* and *in vitro*, synergy with 5-fluorouracil, and safety of recombinant methioninase. Cancer Res. 1998;58:2583–2587. PMID:9635582

[22] Tan Y, Sun X, Xu M, et al. Efficacy of recombinant methioninase in combination with cisplatin on human colon tumors in nude mice. Clin Cancer Res. 1999;5:2157–2163. PMID:10473100

[23] Kokkinakis DM, Hoffman RM, Frenkel EP, et al. Synergy between methionine stress and chemotherapy in the treatment of brain tumor xenografts in athymic mice. Cancer Res. 2001;61:4017–4023. PMID:11358820

[24] Murakami T, Li S, Han Q, et al. Recombinant methioninase effectively targets a Ewing's sarcoma in a patient-derived orthotopic xenograft (PDOX) nude-mouse model. Oncotarget. 2017;8:35630–35638. doi:10.18632/oncotarget.15823. PMID:28404944

[25] Kawaguchi K, Igarashi K, Li S, et al. Combination treatment with recombinant methioninase enables temozolomide to arrest a BRAF V600E melanoma growth in a patient-derived orthotopic xenograft. Oncotarget. 2017;8:85516–85525. doi:10.18632/oncotarget.20231. PMID:29156737

[26] Kawaguchi K, Igarashi K, Li S, et al. Recombinant methioninase (rMETase) is an effective therapeutic for BRAF-V600E-negative as well as -positive melanoma in patient-derived orthotopic xenograft (PDOX) mouse models. Oncotarget. 2018;9:915–923. doi:10.18632/oncotarget.23185. PMID:29416666

[27] Igarashi K, Li S, Han Q, et al. Growth of a doxorubicin-resistant undifferentiated spindle-cell sarcoma PDOX is arrested by metabolic targeting with recombinant methioninase. J Cell Biochem. in press.

[28] Igarashi K Kawaguchi K, Li S, Han Q, et al. Recombinant methioninase in combination with DOX overcomes first-line DOX resistance in a patient-derived orthotopic xenograft nude-mouse model of undifferentiated spindle-cell sarcoma. Cancer Lett. submitted. PMID:29306021

[29] Igarashi K, Kawaguchi K, Kiyuna T, et al. Tumor-targeting Salmonella typhimurium A1-R combined with recombinant methioninase and cisplatinum eradicates an osteosarcoma cisplatinum-resistant lung metastasis in a patient-derived orthotopic xenograft (PDOX) mouse model: Decoy, trap and kill chemotherapy moves toward the clinic. Cell Cycle. submitted.

[30] Kawaguchi K, Han Q, Li S, et al. Targeting methionine with oral recombinant methioninase (o-rMETase) arrests a patient-derived orthotopic xenograft (PDOX) model of BRAF-V600E mutant melanoma: Implications for clinical cancer therapy and prevention. Cell Cycle. in press.

[31] Kawaguchi K, Murakami T, Chmielowski B, et al. Vemurafenib-resistant BRAF-V600E mutated melanoma is regressed by MEK targeting drug trametinib, but not cobimetinib in a patient-derived orthotopic xenograft (PDOX) mouse model. Oncotarget. 2016;7:71737–71743. PMID:27690220

[32] Kawaguchi K, Igarashi K, Murakami T, et al. Tumor-targeting *Salmonella typhimurium* A1-R combined with temozolomide regresses malignant melanoma with a BRAF-V600 mutation in a patient-derived orthotopic xenograft (PDOX) model. Oncotarget. 2016;7:85929–85936.

[33] Kawaguchi K, Igarashi K, Murakami T, et al. Tumor-targeting *Salmonella typhimurium* A1-R sensitizes melanoma with a BRAF-V600E mutation to vemurafenib in a patient-derived orthotopic xenograft (PDOX) nude mouse model. J Cell Biochem. 2017;118:2314–2319. doi:10.1002/jcb.25886. PMID:28106277. PMID:27835903.

[34] Hoffman RM. Patient-derived orthotopic xenografts (PDOX) models of melanoma. Special Issue "Animal Models of Melanoma", Slominski, A., Guest Editor. Intl J Mol Sci. 2017;18:1875. doi:10.3390/ijms18091875.

[35] Hiroshima Y, Zhang Y, Murakami T, et al. Efficacy of tumor-targeting *Salmonella typhimurium* A1-R in combination with anti-angiogenesis therapy on a pancreatic cancer patient-derived orthotopic xenograph (PDOX) and cell line mouse models. Oncotarget. 2014;5:12346–12357.

[36] Fu X, Guadagni F, Hoffman RM. A metastatic nude-mouse model of human pancreatic cancer constructed orthotopically with histologically intact patient specimens. Proc Natl Acad Sci USA. 1992;89:5645–5649. doi:10.18632/oncotarget.2641. doi:10.1073/pnas.89.12.5645. PMID:1608975. PMID:25402324.

[37] Hiroshima Y, Maawy A, Zhang Y, et al. Metastatic recurrence in a pancreatic cancer patient derived orthotopic xenograft (PDOX) nude mouse model is inhibited by neoadjuvant chemotherapy in combination with fluorescence-guided surgery with an anti-CA 19–9-conjugated fluorophore. PLoS One. 2014;9:e114310. doi:10.1371/journal.pone.0114310. PMID:25463150

[38] Hiroshima Y, Maawy AA, Katz MH, et al. Selective efficacy of zoledronic acid on metastasis in a patient-derived orthotopic xenograph (PDOX) nude-mouse model of human pancreatic cancer. J Surg Oncol. 2015;111:311–315. doi:10.1002/jso.23816. PMID:25394368

[39] Fu X, Le P, Hoffma RM. A metastatic-orthotopic transplant nude-mouse model of human patient breast cancer. Anticancer Res. 1993;13:901–904. PMID:8352558

[40] Fu X, Hoffman RM. Human ovarian carcinoma metastatic models constructed in nude mice by orthotopic transplantation of histologically-intact patient specimens. Anticancer Res. 1993;13:283–286. PMID:8517640

[41] Wang X, Fu X, Hoffman RM. A new patient-like metastatic model of human lung cancer constructed orthotopically with intact tissue via thoracotomy in immunodeficient mice. Int J Cancer. 1992;51:992–995. doi:10.1002/ijc.2910510626. PMID:1639545

[42] Hiroshima Y, Zhang Y, Zhang N, et al. Establishment of a patient-derived orthotopic xenograph (PDOX) model of HER-2-positive cervical cancer expressing the clinical metastatic pattern. PLoS One. 2015;10:e0117417. doi:10.1371/journal.pone.0117417. PMID:25689852

[43] Fu X, Besterman JM, Monosov A, et al. Models of human metastatic colon cancer in nude mice orthotopically constructed by using histologically intact patient specimens. Proc Natl Acad Sci USA. 1991;88:9345–9349. doi:10.1073/pnas.88.20.9345. PMID:1924398

[44] Metildi CA, Kaushal S, Luiken GA, et al. Fluorescently-labeled chimeric anti-CEA antibody improves detection and resection of human colon cancer in a patient-derived orthotopic xenograft (PDOX) nude mouse model. J Surg Oncol. 2014;109:451–458. doi:10.1002/jso.23507. PMID:24249594

[45] Hiroshima Y, Maawy A, Metildi CA, et al. Successful fluorescence-guided surgery on human colon cancer patient-derived orthotopic xenograft mouse models using a fluorophore-conjugated anti-CEA antibody and a portable imaging system. J Laparoendosc Adv Surg Tech A. 2014;24:241–247. doi:10.1089/lap.2013.0418. PMID:24494971

[46] Furukawa T, Kubota T, Watanabe M, et al. Orthotopic transplantation of histologically intact clinical specimens of stomach cancer to nude mice: Correlation of metastatic sites in mouse and individual patient donors. Int J Cancer. 1993;53:608–612. doi:10.1002/ijc.2910530414. PMID:8436434

[47] Murakami T, DeLong J, Eilber FC, et al. Tumor-targeting Salmonella typhimurium A1-R in combination with doxorubicin eradicate soft tissue sarcoma in a patient-derived orthotopic xenograft PDOX model. Oncotarget. 2016;7:12783–12790.

[48] Hiroshima Y, Zhao M, Zhang Y, et al. Tumor-targeting Salmonella typhimurium A1-R arrests a chemo-resistant patient soft-tissue sarcoma in nude mice. PLoS One. 2015;10:e0134324. doi:10.18632/oncotarget.7226. doi:10.1371/journal.pone.0134324. PMID:26237416. PMID:26859573.

[49] Kiyuna T, Murakami T, Tome Y, et al. High efficacy of tumor-targeting Salmonella typhimurium A1-R on a doxorubicin- and dactolisib-resistant follicular dendritic-cell sarcoma in a patient-derived orthotopic xenograft PDOX nude mouse model. Oncotarget. 2016;7:33046–33054. doi:10.18632/oncotarget.8848. PMID:27105519

[50] Murakami T, Singh AS, Kiyuna T, et al. Effective molecular targeting of CDK4/6 and IGF-1R in a rare FUS-ERG fusion CDKN2A-deletion doxorubicin-resistant Ewing's sarcoma in a patient-derived orthotopic xenograft (PDOX) nude-mouse model. Oncotarget. 2016;7:47556–47564.

[51] Hiroshima Y, Zhang Y, Zhang N, et al. Patient-derived orthotopic xenograft (PDOX) nude mouse model of soft-tissue sarcoma more closely mimics the patient behavior in contrast to the subcutaneous ectopic model. Anticancer Res. 2015;35:697–701. doi:10.18632/oncotarget.9879. PMID:25667448. PMID:27286459.

[52] Igarashi K, Murakami T, Kawaguchi K, et al. A patient-derived orthotopic xenograft (PDOX) mouse model of an cisplatinum-resistant osteosarcoma lung metastasis that was sensitive to temozolomide and trabectedin: Implications for precision oncology. Oncotarget. 2017;8:62111–62119. doi:10.18632/oncotarget.19095. PMID:28977930

[53] Igarashi K, Kawaguchi K, Kiyuna T, et al. Temozolomide combined with irinotecan caused regression in an adult pleomorphic rhabdomyosarcoma patient-derived orthotopic xenograft (PDOX) nude-mouse model. Oncotarget. 2017;8:75874–75880. doi:10.18632/oncotarget.16548. PMID:29100276

[54] Igarashi K, Kawaguchi K, Murakami T, et al. Intra-arterial administration of tumor-targeting Salmonella typhimurium A1-R regresses a cisplatin-resistant relapsed osteosarcoma in a patient-derived orthotopic xenograft (PDOX) mouse model. Cell Cycle. 2017;16:1164–1170. doi:10.1080/15384101.2017.1317417. PMID:28494180

[55] Murakami T, Kiyuna T, Kawaguchi K, et al. The irony of highly-effective bacterial therapy of a patient-derived orthotopic xenograft (PDOX) model of Ewing's sarcoma, which was blocked by Ewing himself 80 years ago. Cell Cycle. 2017;16:1046–1052. doi:10.1080/15384101.2017.1304340. PMID:28296559

[56] Igarashi K, Kawaguchi K, Murakami T, et al. High efficacy of pazopanib on an undifferentiated spindle-cell sarcoma resistant to first-line therapy is identified with a patient-derived orthotopic xenograft (PDOX) nude mouse model. J Cell Biochem. 2017;118:2739–3743. doi:10.1002/jcb.25923. PMID:28176365

[57] Kiyuna T, Murakami T, Tome Y, et al. Analysis of stroma labeling during multiple passage of a sarcoma imageable patient-derived orthotopic xenograft (iPDOX) in red fluorescent protein transgenic nude mice. J Cell Biochem. 2017;118:3367–3371. doi:10.1002/jcb.25991. PMID:28300287

[58] Igarashi K, Murakami T, Kawaguchi K, et al. A patient-derived orthotopic xenograft (PDOX) mouse model of an cisplatinum-resistant osteosarcoma lung metastasis that was sensitive to temozolomide and trabectedin: Implications for precision oncology. Oncotarget. 2017;8:62111–62119. doi:10.18632/oncotarget.19095. PMID:28977930

[59] Igarashi K, Kawaguchi K, Kiyuna T, et al. Temozolomide combined with irinotecan caused regression in an adult pleomorphic rhabdomyosarcoma patient-derived orthotopic xenograft (PDOX) nude-mouse model. Oncotarget. 2017;8:75874–75880. doi:10.18632/oncotarget.16548. PMID:29100276

[60] Igarashi K, Kawaguchi K, Murakami T, et al. A novel anionic-phosphate-platinum complex effectively targets an undifferentiated pleomorphic sarcoma better than cisplatinum and doxorubicin in a patient-derived orthotopic xenograft (PDOX). Oncotarget. 2017;8:63353–63359. doi:10.18632/oncotarget.18806. PMID:28968995

[61] Miyake K, Murakami T, Kiyuna T, et al. The combination of temozolomide-irinotecan regresses a doxorubicin-resistant patient-derived orthotopic xenograft (PDOX) nude-mouse model of recurrent Ewing's sarcoma with a FUS-ERG fusion and CDKN2A deletion: Direction for third-line patient therapy. Oncotarget. 2017;8:103129–103136. doi:10.18632/oncotarget.20789. PMID:29262551

[62] Yamamoto M, Zhao M, Hiroshima Y, et al. Efficacy of tumor-targeting Salmonella typhimurium A1-R on a melanoma patient-derived orthotopic xenograft (PDOX) nude-mouse model. PLoS One. 2016;11:e0160882. doi:10.1371/journal.pone.0160882. PMID:27500926

[63] Blagosklonny MV. Matching targets for selective cancer therapy. Drug Discov Today. 2003;8:1104–1107. doi:10.1016/S1359-6446(03)02806-X. PMID:14678733

[64] Blagosklonny MV. Teratogens as anti-cancer drugs. Cell Cycle. 2005;4:1518–1521. doi:10.4161/cc.4.11.2208. PMID:16258270

[65] Blagosklonny MV. Treatment with inhibitors of caspases, that are substrates of drug transporters, selectively permits chemotherapy-induced apoptosis in multidrug-resistant cells but protects normal cells. Leukemia. 2001;15:936–941. doi:10.1038/sj.leu.2402127. PMID:11417480

[66] Blagosklonny MV. Target for cancer therapy: Proliferating cells or stem cells. Leukemia. 2006;20:385–391. doi:10.1038/sj.leu.2404075. PMID:16357832

[67] Apontes P, Leontieva OV, Demidenko ZN, et al. Exploring long-term protection of normal human fibroblasts and epithelial cells from chemotherapy in cell culture. Oncotarget. 2011;2:222–233. doi:10.18632/oncotarget.248. PMID:21447859

[68] Blagosklonny MV. Tissue-selective therapy of cancer. Br J Cancer. 2003;89:1147–1151. doi:10.1038/sj.bjc.6601256. PMID:14520435

[69] Suetsugu A, Katz M, Fleming J, et al. Multi-color palette of fluorescent proteins for imaging the tumor microenvironment of orthotopic tumorgraft mouse models of clinical pancreatic cancer specimens. J Cell Biochem. 2012;113:2290–2295. doi:10.1002/jcb.24099. PMID:22573550

[70] Suetsugu A, Katz M, Fleming J, et al. Imageable fluorescent metastasis resulting in transgenic GFP mice orthotopically implanted with human-patient primary pancreatic cancer specimens. Anticancer Res. 2012;32:1175–1180. PMID:22493347

[71] Suetsugu A, Katz M, Fleming J, et al. Non-invasive fluorescent-protein imaging of orthotopic pancreatic-cancer-patient tumorgraft progression in nude mice. Anticancer Res. 2012;32:3063–3068. PMID:22843874

[72] Sun, X, Tan Y, Yang Z, et al. A rapid HPLC method for the measurement of ultra-low plasma methionine concentrations applicable to methionine depletion therapy. Anticancer Res. 2005;24:59–62.